J. Mol. Model. **2000**, *6*, 86 – 98

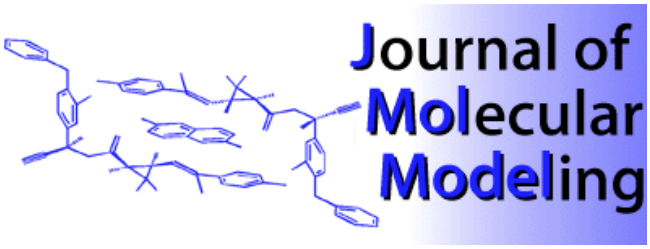

FULL PAPER

Stereochemistry and Stereoelectronics of Azines. 13. Conformational Effects on the Quadrupolarity of Azines. An *Ab Initio* Quantum-Mechanical Study of a Lateral Synthon

Rainer Glaser, Michael Lewis, and Zhengyu Wu

Department of Chemistry, University of Missouri-Columbia, Columbia, Missouri 65211 USA. Tel.: (573) 882-0331; Fax: (573) 882-2754. E-mail: GlaserR@missouri.edu

Received: 15 October 1999/ Accepted: 17 December 1999/ Published: 28 February 2000

Abstract The quadrupole moment of formaldazine, H_2C=N-N=CH_2, has been studied for the *trans* structure ($\angle$(C-N-N-C) = τ = 180º) and a series of *gauche* structures (τ > 120º). Restricted Hartree-Fock theory, second-order Møller-Plesset theory, and quadratic CI theory have been used in conjunction with the basis sets 6-31G*, 6-31G**, 6-311G** and 6-311++G**. Formaldazine is a quadrupolar molecule with primitive quadrupole moment tensor components of Q_{xx} = -22.4, Q_{yy} = -20.4 and Q_{zz} = -25.6 DÅ at the theoretical level QCISD/6-311++G**. The examination of the theoretical level dependency shows that the reliable computation of a quadrupole moment requires the use of a flexible basis set. A large part of the component Q_{zz} = -25.6 DÅ is due to the π-system and compares, on a per electron basis, with the Q_{zz} value of benzene. Conformational changes of the azines in the range 120° < τ < 180º have but a minute effect on the energy and are associated with only minor electronic relaxation. These conformational changes alter the quadrupole moment tensor components less than ΔQ_{xx} = +0.4, ΔQ_{yy} = +1.6 and ΔQ_{zz} = -1.0 DÅ at QCISD/6-311++G**//QCISD/6-31G*. The direction of these changes is explained by consideration of the rotation of the CN-π-systems and a small reduction of the CN bond polarity in the *gauche* structures. The Q_{zz} component of formaldazine is representative of the quadrupole moment tensor component along the direction of the C_2 axis of the azine bridge as such. Hence, the results of this study suggest that azines can engage in strong quadrupole-quadrupole interactions and can be employed as lateral synthons in crystal engineering.

Keywords Quadrupole, Azine, Potential energy surface analysis, Conformational analysis, Synthon, Crystal engineering

Introduction

We have been interested in the orientational order of polar molecules in the solid state and it is one of our goals in this area to achieve the complete parallel alignment of dipolar molecules in a rational manner. This goal is a rather ambi-

Correspondence to: R. Glaser

Dedicated to Professor Paul Ragué von Schleyer on the occasion of his 70th birthday

tious one considering that the overwhelming majority of polar molecules crystallize with dipole moment cancellation resulting in nonpolar crystals. Polar crystals tend to result from the incomplete cancellation of dipole moments where μ(crystal) « $\Sigma\mu$(molecule). There are only very few molecular crystals where the molecules pack such that the dipole moments are almost perfectly parallel, notably the crystal structures of DAD [1], MAP [2], APDA [3], and DMACB [4], and there has been little effort aimed at understanding why these crystals pack in such a remarkable fashion. We have been investigating azines with the general formula D–Ph–C(Me)=N–N=C(Me)–Ph–A where D and A are electron donors and acceptors, respectively [5,6]. In two instances (D = OMe, A = Br; and D = OMe, A = Cl) the azine molecules pack to afford near–perfect dipole–parallel aligned crystals [5]. The azines were designed in a way that should *facilitate* parallel-dipole alignment in the pure crystal. With the realization of two prototypes, it is now one of our primary goals to understand in detail the intermolecular interactions responsible for this unique packing arrangement. We performed numerical simulations which showed that parallel dipole alignment may correspond to a local minimum on the potential energy surface of a hypothetical crystal consisting solely of point dipoles [7]. For one path, we showed that there is a sizeable activation barrier associated with the interconversion between antiparallel and parallel dipole moment alignment. The global minimum of this dipole lattice is the antiparallel aligned motif and this cannot be changed. However, by introduction of additional intermolecular interactions that further stabilize the dipole–parallel aligned motif, we will increase our chances of obtaining crystals with parallel aligned dipole moments. Hence, our research focuses on the exploration of strategies that provide high degrees of intermolecular attraction of parallel oriented and parallel positioned molecules. Fragments with high quadrupole moment components perpendicular to the oriented dipolar axis are being explored as promising candidates for such lateral synthons.

It was one of our original design concepts to incorporate arene–arene contacts as a tool for stabilizing the dipole–parallel aligned packing motif. The validity and usefulness of this concept has been confirmed and one of the predominant intermolecular interactions in most of our azine crystals is the arene–arene double T–contact [5,6,8]. A double T–contact occurs when the two phenyl rings of one azine interact with the two phenyl rings of an adjacent azine to give two T–contacts. Thus, an area of intensive current research in our group is directed toward quantification of the energetics of these double T–contacts *via* quantum-mechanical *ab initio* methods. Besides the double T–contact, an unexpected intermolecular interaction also is predominant in most of our azine crystals, and this interaction is between the azine spacer and a phenyl ring (Figure 1). This interaction comes in a great variety of flavors since the contact can be face-to-face or T-shaped and since the contact may occur with offsets. The azine adds an additional variable through its conformational flexibility. A detailed discussion of the many structural options of azine-arene contacts will be given elsewhere and two examples may provide a glimpse at this manifold. The X-ray structure of the MeO-H_4C_6-CMe=N-N=CMe-C_6H_4-Cl, shown in parts (a) – (d), features a distorted azine – benzene T-contact [5a]. The X-ray structure of F_5C_6-CH=N-N=CH-C_6F_5, shown in parts (d) – (e), features an offset face-to-face contact between an azine and benzene [9].

While the literature contains many examples of arene–arene contacts [10,11] and numerous studies that suggest that the attraction results from quadrupole–quadrupole interactions [12,13] the literature is devoid of any discussions of

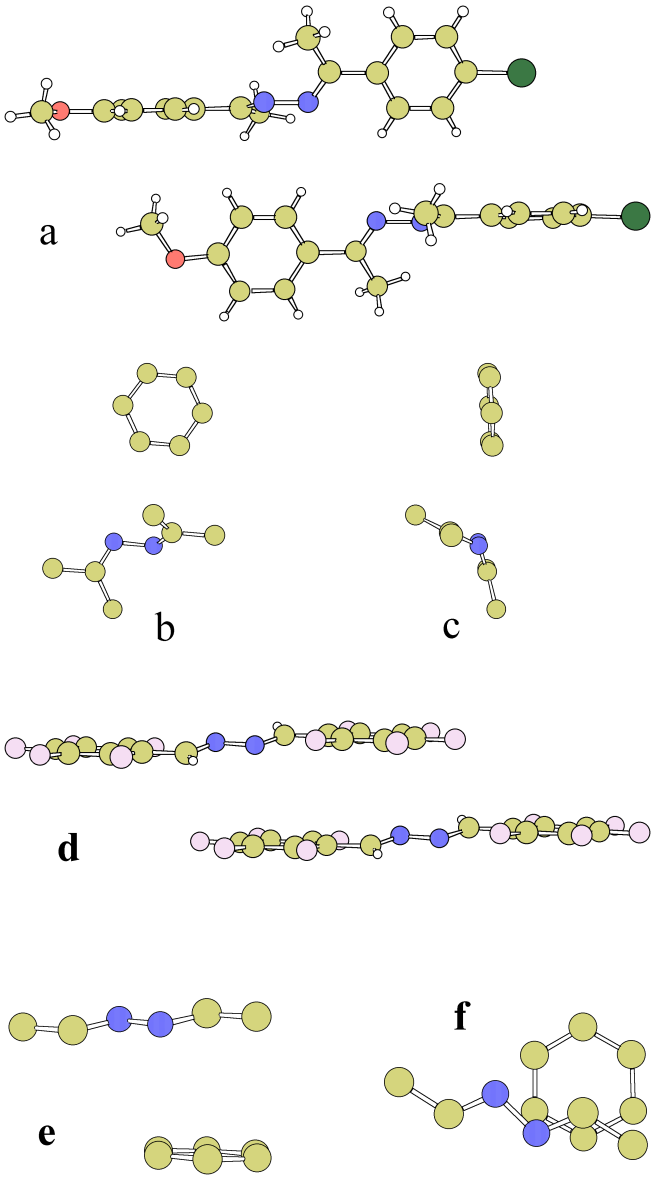

Figure 1 *The X-ray structure of the MeO-H_4C_6-CMe=N-N=CMe-C_6H_4-Cl, shown in parts (a) – (d), features a distorted azine – benzene T-contact. The X-ray structure of the F_5C_6-CH=N-N=CH-C_6F_5, shown in parts (d) – (e), features a face-to-face contact between an azine bridge and benzene*

Table 1 *Structures of Formaldazine in the* trans *Conformation, ∠(C-N-N-C) = 180°*

Theoretical Model	NN	NC	HC 1	HC 2	CNN	HCN 1	HCN 2	HCNN 1	HCNN 2
RHF/									
6-31G*	1.396	1.253	1.076	1.079	112.3	118.3	122.6	180.0	0.0
6-31G**	1.396	1.253	1.077	1.080	112.3	118.3	122.4	180.0	0.0
6-311G**	1.393	1.251	1.077	1.081	112.5	118.3	122.2	180.0	0.0
6-311++G**	1.391	1.252	1.077	1.081	112.8	118.3	122.2	180.0	0.0
MP2(full)/									
6-31G*	1.429	1.285	1.086	1.090	110.0	117.7	122.5	180.0	0.0
6-31G**	1.430	1.285	1.081	1.085	109.9	117.7	122.4	180.0	0.0
6-311G**	1.420	1.282	1.086	1.091	110.2	117.6	121.7	180.0	0.0
6-311++G**	1.418	1.284	1.086	1.091	110.7	117.5	121.9	180.0	0.0
QCISD/									
6-31G* := Q	1.434	1.282	1.089	1.093	110.3	117.9	122.6	180.0	0.0
6-31G**	1.434	1.282	1.083	1.087	110.2	117.9	122.6	180.0	0.0
6-311G**	1.426	1.279	1.088	1.093	110.5	117.8	122.1	180.0	0.0
6-311++G**	1.423	1.280	1.088	1.093	110.9	117.8	122.2	180.0	0.0

[a] Distances are given in Å and angles in degrees.
[b] All electrons were included in the perturbation calculations, MP2(full). The core electrons were frozen in the QCISD calculations, QCISD(fc).

Table 2 *Structures of Formaldazine in the Conformation with ∠(C-N-N-C) = 160°*

Theoretical Model	NN	NC	HC 1	HC 2	CNN	HCN 1	HCN 2	HCNN 1	HCNN 2
RHF/									
6-31G*	1.394	1.253	1.076	1.079	112.6	118.3	122.6	180.5	0.6
6-31G**	1.394	1.253	1.077	1.080	112.6	118.3	122.5	180.5	0.6
6-311G**	1.392	1.250	1.077	1.081	112.7	118.3	122.3	180.5	0.7
6-311++G**	1.390	1.251	1.077	1.081	113.0	118.3	122.3	180.5	0.6
MP2(full)/									
6-31G*	1.427	1.285	1.086	1.090	110.3	117.7	122.7	180.5	0.5
/6-31G**	1.426	1.284	1.081	1.086	110.2	117.6	122.5	180.5	0.5
/6-311G**	1.418	1.282	1.086	1.091	110.5	117.5	122.0	180.6	0.6
/6-311++G**	1.415	1.284	1.086	1.091	110.9	117.5	122.0	180.3	0.6
QCISD/									
6-31G* := Q	1.432	1.282	1.089	1.093	110.5	117.9	122.8	180.5	0.5

[a] See legend to Table 1

arene–azine contacts. Moreover, the quadrupole moments of azines are not known. Therefore, in this paper we present a higher level *ab initio* study of the quadrupole moment of the parent azine, formaldazine $H_2C{=}N{-}N{=}CH_2$, using various quantum-mechanical methods and a variety of basis sets. The C-N-N-C dihedral angles of the azine bridge in our crystal structures vary from 125° to 180° and thus we studied the conformational effects on the quadrupole moment of the parent azine for C-N-N-C dihedral angles τ of 120°, 140°, 160° and 180°.

Table 3 *Structures of Formaldazine in the Conformation with ∠(C-N-N-C) = 140°*

Theoretical Model	NN	NC	HC 1	HC 2	CNN	HCN 1	HCN 2	HCNN 1	HCNN 2
RHF/									
6-31G*	1.391	1.252	1.076	1.079	112.6	118.3	122.9	180.3	0.5
6-31G**	1.390	1.252	1.076	1.080	113.4	118.2	122.8	180.3	0.6
6-311G**	1.388	1.249	1.077	1.081	113.6	118.2	122.6	180.4	0.6
6-311++G**	1.387	1.250	1.077	1.081	113.0	118.2	122.6	180.3	0.6
MP2(full)/									
6-31G*	1.419	1.284	1.086	1.091	110.3	117.6	123.0	180.2	0.3
6-31G**	1.419	1.284	1.081	1.086	111.1	117.6	122.8	180.2	0.3
6-311G**	1.410	1.282	1.085	1.091	111.4	117.4	122.4	180.3	0.5
6-311++G**	1.408	1.283	1.085	1.092	110.9	117.4	122.4	180.1	0.5
QCISD/									
6-31G* := Q	1.425	1.281	1.088	1.093	110.5	117.8	123.0	180.3	0.4

[a] See legend to Table 1

Table 4 *Structures of Formaldazine in the Conformation with ∠(C-N-N-C) = 120°*

Theoretical Model	NN	NC	HC 1	HC 2	CNN	HCN 1	HCN 2	HCNN 1	HCNN 2
RHF/									
6-31G*	1.383	1.250	1.076	1.080	114.9	118.2	123.1	179.3	-0.5
6-31G**	1.383	1.250	1.076	1.081	115.0	118.2	123.0	179.2	-0.5
6-311G**	1.381	1.248	1.077	1.082	115.1	118.2	122.9	179.3	-0.3
6-311++G**	1.380	1.249	1.077	1.082	115.2	118.1	122.8	179.4	-0.1
MP2(full)/									
6-31G*	1.405	1.284	1.085	1.091	113.0	117.5	123.3	178.9	-1.0
6-31G**	1.404	1.283	1.080	1.086	112.9	117.5	123.2	178.9	-1.0
6-311G**	1.396	1.282	1.085	1.092	113.2	117.3	122.8	179.0	-0.7
6-311++G**	1.396	1.283	1.085	1.092	113.4	117.4	122.7	179.1	-0.5
QCISD/									
6-31G* := Q	1.413	1.281	1.088	1.094	113.0	117.7	123.3	179.1	-0.7

[a] See legend to Table 1

Theoretical methods and computations

The elements Q_{ij} of the quadrupole moment tensor are defined as

$$Q_{ij} = \int \sigma(\mathbf{r})\, r_i r_j\, d\mathbf{r} \qquad (i = x, y, z) \tag{1}$$

where $\sigma(\mathbf{r})$ is the charge density distribution and r_i and r_j are the components of the distance vector (x, y, z) from the molecular center of nuclear charge. Alternatively, one might separate the terms that are caused by the n nuclei with their nuclear charges $Z(n)$ and the electron density distribution $\rho(\mathbf{r})$ and the expression for the tensor elements becomes

$$Q_{ij} = \Sigma\, Z(n)\, r_i(n) r_j(n) - \int |\rho(\mathbf{r})|\, r_i r_j\, d\mathbf{r} \tag{2}$$

and for the diagonal elements this equation reduces to the form

$$Q_{ii} = \Sigma\, Z(n)\, r_i(n)^2 - \int |\rho(\mathbf{r})|\, r_i^2\, d\mathbf{r} \tag{3}$$

Table 5 *Energies of Formaldazine in the* trans *Conformation as a Function of the Dihedral Angle ∠(C-N-N-C) = τ*

Theoretical Model	Energy τ = 180°	Energy τ = 160°	Energy τ = 140°	Energy τ = 120°
RHF/				
6-31G*	-186.885997	-186.885334	-186.883632	-186.881799
6-31G**	-186.892867	-186.892204	-186.890500	-186.888658
6-311G**	-186.933212	-186.932515	-186.930723	-186.928734
6-311++G**	-186.937238	-186.936582	-186.934777	-186.932597
MP2(full)/				
6-31G*	-187.473297	-187.473026	-187.472379	-187.471900
6-31G**	-187.505526	-187.505261	-187.504632	-187.504182
6-311G**	-187.629050	-187.628842	-187.628332	-187.627960
6-311++G**	-187.638491	-187.638451	-187.637975	-187.637220
QCISD/				
6-31G* := Q	-187.489744	-187.489469	-187.488761	-187.488032
6-31G**	-187.521945			
6-31G**//Q	-187.521851	-187.521582	-187.520893	-187.520190
6-311G**	-187.585423			
6-311G**//Q	-187.585330	-187.585102	-187.584488	-187.583821
6-311++G**	-187.593447			
6-311++G**//Q	-187.593334	-187.593260	-187.592699	-187.591713

[a] Total energies are given in atomic units
[b] All electrons were included in the perturbation calculations, MP2(full). The core electrons were frozen in the QCISD calculations, QCISD(fc)

Table 6 *Relative Energies of Formaldazine as a Function of the Dihedral Angle ∠(C-N-N-C)*

Theoretical Model	160°	140°	120°
RHF/6-31G*	0.42	1.48	2.63
RHF/6-31G**	0.42	1.49	2.64
RHF/6-311G**	0.44	1.56	2.81
RHF/6-311++G**	0.41	1.54	2.91
MP2(full)/6-31G*	0.17	0.58	0.88
MP2(full)/6-31G**	0.17	0.56	0.84
MP2(full)/6-311G**	0.13	0.45	0.68
MP2(full)/6-311++G**	0.02	0.32	0.80
QCISD/6-31G* := Q	0.17	0.62	1.07
QCISD/6-31G**//Q	0.17	0.60	1.04
QCISD/6-311G**//Q	0.14	0.53	0.95
QCISD/6-311++G**//Q	0.05	0.40	1.02

[a] Relative energy in kcal·mol^{-1} with respect to the trans *structure*

The off-diagonal tensor elements Q_{ij} vanish whenever the molecule has a plane of symmetry perpendicular to either one of the coordinates *i* and *j*. We chose the orientation of the azines as depicted in Scheme 1. The C_2-axis of the molecule is aligned with the *z*-axis and the N-N bond is colinear with the *x*-axis. For the *trans* conformation it is obvious that Q_{xz} and Q_{yz} vanish because the *xy*-plane is a symmetry plane. These terms also vanish because of the C_2-axis. The C_2-axis transforms (*x, y, z*) into (*-x, -y, z*) and integrals containing $r_i r_j$ will vanish whenever the symmetry operation leads to an odd number of sign changes. Thus, for all conformations of formaldazine, the non-zero elements are the diagonal elements Q_{ii} and the off-diagonal element Q_{xy}.

The determination of the quadrupole moment tensor requires the electron density distribution $\rho(r)$ for a given nuclear configuration. We have determined electron density functions $\rho(r)$ using several theoretical methods [14]. Restricted Hartree-Fock (RHF) theory is the obvious starting point. RHF theory includes only a part of the electron correlation between same spin electrons and post-HF methods need to be employed to more fully account for electron correlation. We have employed both Møller-Plesset perturbation theory and quadratic configuration interaction theory to that effect. Both of these methods are size-consistent. All single and double excitations were included in the perturbation calculations and the active space of these second-order Møller-Plesset calculations included all electrons and all molecular orbitals, MP2(full). The quadratic CI theory [15] is the most sophisticated theory applied here. In this advanced method, the RHF reference wavefunction is used as the starting point of a variational configuration interaction calculation that includes single and double excitations, QCISD. The

Table 7 *Quadrupole Moment Tensor Components of Formaldazine in the* trans *Conformation, ∠(C-N-N-C) = 180°*

Theoretical Model	Q_{xx}	Q_{yy}	Q_{zz}	Q_{xy}	Q_{xx}-Q_{zz}	Q_{yy}-Q_{zz}
RHF/						
6-31G*	-21.559	-19.344	-24.958	-5.417	3.399	5.614
6-31G**	-21.531	-19.376	-24.940	-5.372	3.409	5.564
6-311G**	-21.535	-19.641	-25.110	-5.386	3.575	5.469
6-311++G**	-21.826	-19.727	-25.511	-5.657	3.684	5.783
MP2(full)/						
6-31G*	-21.834	-18.863	-25.259	-5.494	3.426	6.396
6-31G**	-22.072	-19.952	-24.840	-4.924	2.768	4.888
6-311G**	-22.147	-20.438	-25.170	-4.925	3.023	4.733
6-311++G**	-22.079	-19.279	-25.836	-5.708	3.758	6.558
QCISD/						
6-31G* := Q	-21.947	-19.779	-24.908	-5.041	2.962	5.130
6-31G**	-22.065	-19.946	-24.812	-4.936	2.747	4.866
6-31G**//Q	-22.059	-19.963	-24.842	-4.935	2.783	4.879
6-311G**	-22.109	-20.367	-25.092	-4.939	2.983	4.725
6-311G**//Q	-22.152	-20.270	-25.119	-4.984	2.967	4.849
6-311++G**	-22.486	-20.459	-25.610	-5.382	3.125	5.152
6-311++G**//Q	-22.597	-20.333	-25.631	-5.391	3.034	5.298

[a] All quadrupole moment tensor components are given in DÅ

Table 8 *Quadrupole Moment Tensor Components of Formaldazine in the Conformation with ∠(C-N-N-C) = 160°*

Theoretical Model	Q_{xx}	Q_{yy}	Q_{zz}	Q_{xy}	Q_{xx}-Q_{zz}	Q_{yy}-Q_{zz}
RHF/						
6-31G*	-21.528	-19.565	-24.802	-5.310	3.274	5.237
6-31G**	-21.501	-19.592	-24.787	-5.266	3.286	5.194
6-311G**	-21.504	-19.843	-24.968	-5.281	3.464	5.124
6-311++G**	-21.781	-19.925	-25.361	-5.560	3.579	5.436
MP2(full)/						
6-31G*	-21.927	-19.986	-24.791	-4.927	2.864	4.806
6-31G**	-22.042	-20.150	-24.712	-4.814	2.670	4.562
6-311G**	-22.116	-20.617	-25.060	-4.813	2.945	4.443
6-311++G**	-22.542	-20.722	-25.658	-5.304	3.116	4.936
QCISD/						
6-31G* := Q	-21.915	-19.979	-24.772	-4.931	2.857	4.793
6-31G**//Q	-22.028	-20.154	-24.713	-4.826	2.685	4.559
6-311G**//Q	-22.119	-20.448	-25.002	-4.876	2.883	4.555
6-311++G**//Q	-22.547	-20.517	-25.504	-5.286	2.956	4.987

[a] See legend to Table 7

Table 9 *Quadrupole Moment Tensor Components of Formaldazine in the Conformation with ∠(C-N-N-C) = 140°*

Theoretical Model	Q_{xx}	Q_{yy}	Q_{zz}	Q_{xy}	Q_{xx}-Q_{zz}	Q_{yy}-Q_{zz}
RHF/						
6-31G*	-21.427	-20.193	-24.378	-4.990	2.951	4.185
6-31G**	-21.401	-20.211	-24.368	-4.951	2.967	4.157
6-311G**	-21.402	-20.422	-24.580	-4.969	3.178	4.159
6-311++G**	-21.661	-20.519	-24.939	-5.251	3.278	4.420
MP2(full)/						
6-31G*	-21.813	-20.573	-24.420	-4.608	2.607	3.847
6-31G**	-21.931	-20.710	-24.364	-4.500	2.433	3.654
6-311G**	-22.010	-21.122	-24.763	-4.494	2.753	3.641
6-311++G**	-22.411	-21.270	-25.321	-4.969	2.909	4.051
QCISD/						
6-31G* := Q	-21.803	-20.547	-24.398	-4.622	2.595	3.851
6-31G**//Q	-21.921	-20.697	-24.362	-4.522	2.441	3.665
6-311G**//Q	-22.005	-20.953	-24.680	-4.571	2.674	3.727
6-311++G**//Q	-22.402	-21.060	-25.142	-4.977	2.739	4.082

[a] See legend to Table 7

Table 10 *Quadrupole Moment Tensor Components of Formaldazine in the Conformation with ∠(C-N-N-C) = 120°*

Theoretical Model	Q_{xx}	Q_{yy}	Q_{zz}	Q_{xy}	Q_{xx}-Q_{zz}	Q_{yy}-Q_{zz}
RHF/						
6-31G*	-21.235	-21.108	-23.810	-4.495	2.574	2.702
6-31G**	-21.211	-21.116	-23.806	-4.461	2.595	2.690
6-311G**	-21.215	-21.272	-24.056	-4.487	2.842	2.785
6-311++G**	-21.470	-21.413	-24.359	-4.747	2.888	2.946
MP2(full)/						
6-31G*	-21.588	-21.428	-23.926	-4.126	2.338	2.498
6-31G**	-21.712	-21.525	-23.905	-4.025	2.193	2.380
6-311G**	-21.800	-21.864	-24.362	-4.015	2.562	2.498
6-311++G**	-22.188	-22.088	-24.853	-4.442	2.665	2.765
QCISD/						
6-31G*	-21.595	-21.377	-23.887	-4.158	2.292	2.510
6-31G**//Q	-21.720	-21.489	-23.884	-4.065	2.164	2.394
6-311G**//Q	-21.798	-21.701	-24.230	-4.117	2.432	2.529
6-311++G**//Q	-22.167	-21.879	-24.630	-4.490	2.463	2.751

[a] See legend to Table 7

active space included all valence electrons and the entire virtual space while the four core molecular orbitals were kept frozen. Several basis sets were employed in conjunction with these three methods. The smallest of these basis sets was the 6-31G* basis set [16]. Split-valence basis sets are required to allow for anisotropies at the atoms and these are especially important in computations of quadrupole moment tensor elements. The inclusion of polarization functions in the basis set is mandatory to account for the reduced symmetry of the atomic orbitals in the molecules. The three other basis

Table 11 *NPA Charges of Formaldazine as a Function of the Dihedral Angle ∠(C-N-N-C). All Calculations are at QCISD/6-311++G**// QCISD/6-31G**

∠(C-N-N-C)	N	C	H1	H2
180°	-0.306	-0.003	0.158	0.151
160°	-0.302	-0.006	0.159	0.150
140°	-0.291	-0.016	0.159	0.148
120°	-0.275	-0.030	0.160	0.144

sets employed are 6-31G**, 6-311G** and 6-311++G** [16,17 ,18]. Polarization functions on the H-atoms were added first; this change has only minor consequences since the polarization of H-atoms is in part accomplished already by the basis sets on the adjacent heavy atom. The step from a double-ζ to triple-ζ valence description is a major improvement. The addition of the diffuse functions might further refine the electron density distribution especially with a view to the π-density and the lone pairs. The larger basis sets are especially advantageous in that they provide improved virtual spaces in the correlation treatments. As far as the geometries are concerned, one has several options to consider. To use the experimental structure in one's calculation is an option so long as one is interested only in observable systems. In conformational analysis one commonly employs the structure that is optimal for a given dihedral angle at a given theoretical level. Hence, we have optimized all structures at the RHF and MP2(full) levels with each of the basis sets. The structural optimizations at the QCISD level are rather computer-time intensive even if one has an 8-node minisupercomputer at one's disposal. We still optimized the *trans* structures at all of the QCISD levels but we adopted a modified and more modest strategy for the other conformations. The structures of formaldazine were optimized at the QCISD/6-31G* level for each value of τ but no further structure optimizations were carried out in the QCISD calculations with the more extended and augmented basis sets. These calculations are referred to as single point calculations and following a notation introduced by Pople they are denoted by specification of the theoretical methods used for the calculation of the wave function (at the higher theoretical level) and of the structure optimization (at QCISD/6-31G*) and separated by a "//". The data in Table 5 show the similarity between the QCISD/6-311++G** and QCISD/6-311++G**//QCISD/6-31G* results and they provide a justification for the approach. One of the arguments we will advance below relies on the results of a Natural Bond Orbital (NBO) population analysis [19]. This analysis was carried out at one level only and the highest theoretical level was selected, that is, we employed the QCI electron density obtained in the QCISD/6-311++G**// QCISD/6-31G* calculations.

The *ab initio* calculations were carried out with the program Gaussian94 [20] on a Silicon Graphics PowerChallenge L minisupercomputer. Optimized structures are documented in Tables 1 – 4. Total and relative energies are summarized in Tables 5 and 6. The calculated primitive quadrupole moment tensor components of formaldazine are summarized in Tables 7 - 10. The results of the NBO analysis are given in Table 11.

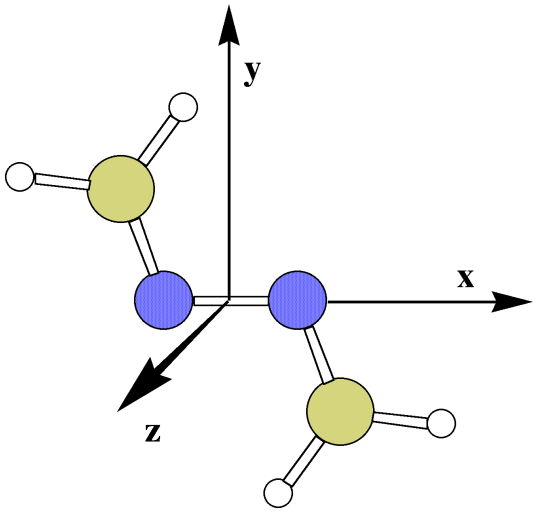

Scheme 1 *Orientation of the formaldazines. The z-axis coincides with the C_2 axis and the x-axis is colinear with the NN bond*

Results and discussion

Potential energy surface of formaldazine

IR and Raman studies [21] and an electron diffraction [22] study show that formaldazine exists "as a mixture of s-*trans* and [*cis*-] *gauche* conformers with the *trans* the more stable" (75% *trans* at 225 °C). Vibrational spectroscopy shows that acetone azine assumes the N-N *trans* conformation (C_{2h}) [23 a] and PE spectroscopy [23b] suggests the same conformation also for alkyl azines. The N-N rotational profile was discussed by Shancke [24] (RHF/DZ), Bock *et al.* [25] (RHF/6-31G*), Bachrach and Liu [26] (MP2/6-31G*//RHF/6-31G*), Oberhammer *et al.* [27] (MP2/6-31G**//RHF/6-31G**), and Wiberg *et al.* [28] (MP3/6-311++G**//MP2/6-31*). These studies consistently show that the potential energy surface is rather flat in the *gauche* region. The best estimate for the relative energy of *cis* compared to *trans* formaldazine is 15.9 kcal·mol^{-1} and the g*auche* region is about 2 kcal·mol^{-1} less stable than the *trans* conformation.

Theory and experiment thus agree that the *trans* structure is the most stable, that the *cis* conformation is a transition state significantly higher in energy, and that a wide region

between 180° > τ > 90° is only modestly higher in energy than the *trans* conformation. Crystallography can contribute to the discussion of the N-N conformation in that the crystallographic record shows but little of an energetic advantage for the *trans* conformation with τ = 180°: As many substituted azines realize *gauche* conformations with 115° < τ < 150° as there are known *trans* structures [29]. Moreover, it is known from *ab initio* studies of substituted azines that they may exhibit a small intrinsic *gauche* preference [30].

We optimized the structure of formaldazine as a function of the dihedral angle τ using the RHF, MP2(full) and QCISD methods in conjunction with the basis sets 6-31G*, 6-31G**, 6-311G** and 6-311++G**. The results are documented in Tables 1 – 6. The data are in line with the previous studies and, in particular, the use of the most sophisticated QCISD levels reaffirm the flat shape of the rotational energy profile.

Quadrupole moment tensor components of formaldazine

The non-zero quadrupole moment tensor components of formaldazine are given in Tables 7 – 10. The quadrupole moment tensor is dominated by the diagonal elements and all of these are negative. Negative Q_{ii} values indicate that, on r^2-weighted average, the negative charge distribution is farther removed from the molecular center of the nuclear charges. Hence, in all three independent directions all conformations of formaldazine are characterized by the quadrupolarity {- + -}.

The drawings in Scheme 2 may serve to illustrate graphically the origins of the diagonal quadrupole tensor moments for benzene and formaldazine. The negative sign of Q_{zz} is relatively easily understood. Moving through a π-system perpendicular to the molecular plane one first encounters the negative region of the π-cloud, then the positive area of the nuclei, and then the second negative region of the π-cloud. The {- + -} quadrupolarity Q_{zz} is thus intuitively easy to grasp and $Q_{zz} < 0$ has to result since the nuclei do not contribute to Q_{zz} at all. It is important to realize that Q_{zz} is not only a function of the π-molecular orbitals but also contains contributions from the σ-molecular orbitals. The latter are neglected in the drawings in Scheme 2, parts (a) and (b), but we will see later that the contributions of the σ-molecular orbitals to Q_{zz} actually are quite sizeable. To rationalize the quadrupole moment tensor components Q_{xx} and Q_{yy} is more involved and we consider benzene first (Scheme 2, part (c)). The polarity of the C-H bond in benzene is well known; the H-atom is the *positive* pole [31]. This knowledge might lead one to suspect

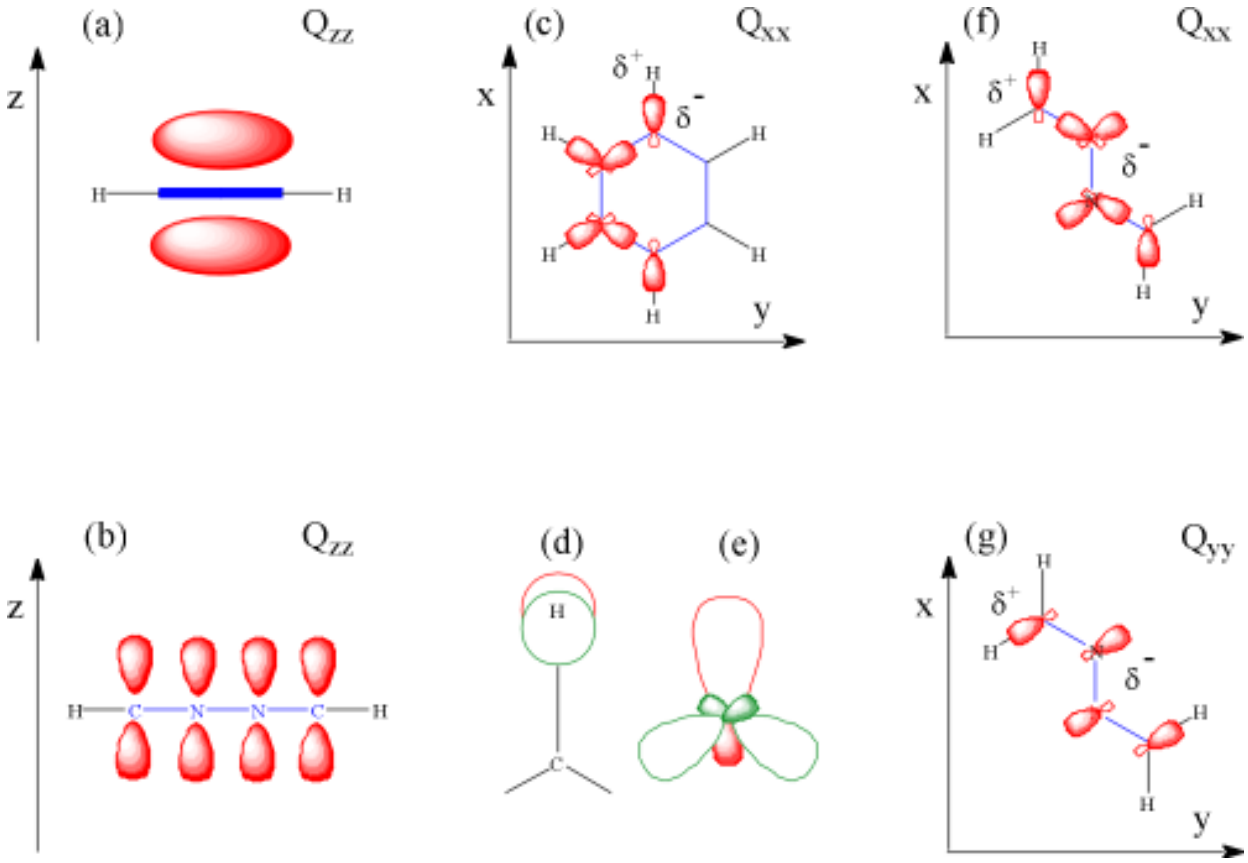

Scheme 2 *Illustrations providing qualitative rational for the origins of the signs of the computed quadrupole moment tensors. See text for discussion*

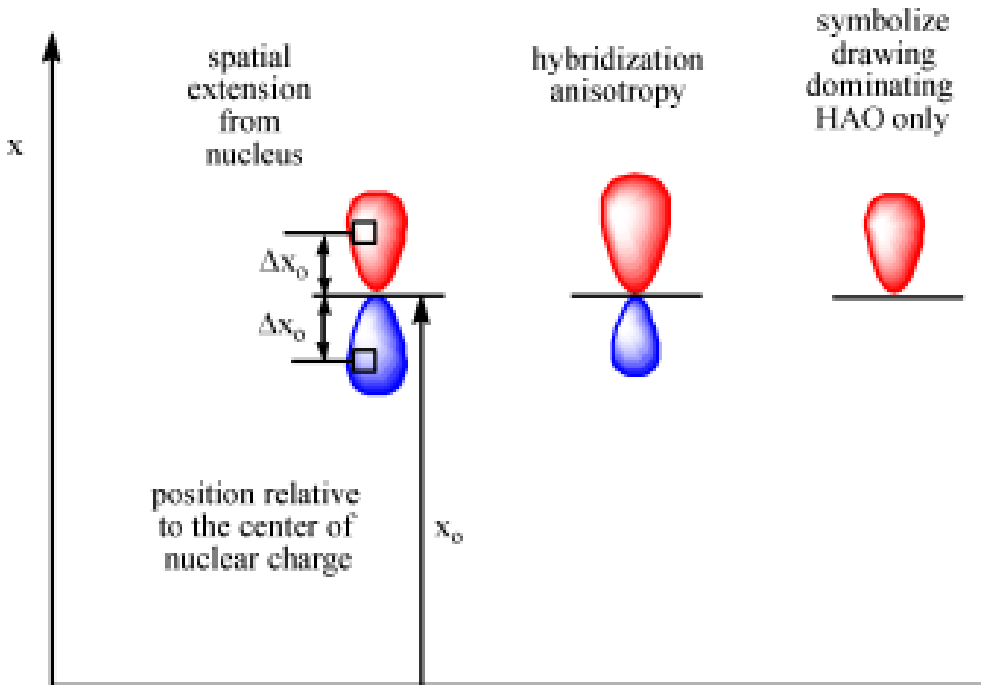

Scheme 3 *Illustration of the factors determining quadrupole moment tensor components. Two sp_x hybrid orbitals are shown in red and blue*

that Q_{xx} would be a *positive* number. Clearly, the electron density originally associated with the H-atom is shifted toward the C-atom (Scheme 2, part (d)) and this shift has to give a positive contribution to the quadrupole moment tensor element Q_{xx}. Which feature of the electron density distribution about the C-atom is it, then, that causes a *negative* and dominant contribution to the quadrupole moment tensor element Q_{xx}? Consider the electron density distributions associated with two degenerate sp_x hybrid orbitals centered at a distance x_o from the molecular center of nuclear charge. The positions $x_o+\Delta x$ and $x_o-\Delta x$ are equidistant from the position x_o. The volume elements of electron density at the positions $x_o-\Delta x$ and $x_o+\Delta x$, respectively, contribute $-|\rho(\boldsymbol{r})| \cdot (x_o-\Delta x)^2$ and $-|\rho(\boldsymbol{r})| \cdot (x_o+\Delta x)^2$, respectively, and the combined contribution of these two volume elements to Q_{xx} is $-|\rho(\boldsymbol{r})| \cdot (2x_o^2+2\Delta x^2)$. An atom-centered electron density component that is symmetrical with regard to that atom contributes to Q_{xx} and the contribution increases (i) with the distance of the atom from the center of nuclear charge and (ii) with the spatial extension of the orbital (influences how large Δx can become). This is illustrated in Scheme 3. At the next level of sophistication one might consider differences in the shapes of the approximate sp hybrid orbitals. One of the hybrid orbitals might be more spatially extended and this "hybridization anisotropy" is illustrated to the right in Scheme 3. A similar and slightly more involved consideration applies to sets of sp^2 hybrid orbitals and we want to provide an example for the "hybridization anisotropy" by consideration of the C-C and C-H σ bonds. The C-sp^2-type hybrid orbital of the C-H bond is spatially more extended than the respective C-sp^2-type hybrid orbital of the CC bonds (Scheme 2, part (e)). This statement makes physical sense because the electrons involved in CC bonding are more contracted due to the higher attraction term in the one-electron core Hamiltonian of the CC bonding MO. Extended basis sets are required to adequately describe this C-atom anisotropy because the greater spatial extension of the C-density in the C-H bonding region requires the use of greater contribution of the outer C-p-basis function(s). The quadrupolarity Q_{xx} can therefore be understood as the result of three effects: (i) atom positioning x_o, (ii) hybrid orbital spatial extension Δx and (iii) hybridization anisotropy. These insights suggest a simple graphical notation for the discussion of the origin of quadrupole moments. For all atom-centered sets of C-sp^2-type hybrid orbital, we draw only the one(s) that is (are) oriented away from the center of nuclear charge and its (their) direction will indicate this atom's contribution to the electronic quadrupole moment component. The tensor moments Q_{xx} and Q_{yy} of the azine can be understood with similar considerations. As with benzene, the negative sign of Q_{xx} might seem to run counter-intuitive to the polarity of the CN bonds. The N-atoms are negatively charged and the methylene H-atoms carry positive charge. In the case of the azine, the Q_{xx} and Q_{yy} tensor components contain contributions due to C- and N-atoms and, in parts (f) and (g) of Scheme 2, we have drawn just those sp^2-hybrid orbitals that are most removed from the center of nuclear charge.

The quadrupole moment tensor component Q_{zz} of formaldazine is about –25 DÅ and it can be compared to the value of –40 DÅ in benzene [32,33]. The contribution per p_z-orbital in benzene is -6.7 DÅ while the respective number for the azine is -6.3 DÅ. This slightly reduced magnitude reflects the compactness of the N-p(π)-orbitals. The quadrupole moment tensor components Q_{xx} and Q_{yy} are smaller by about 3 and 5 DÅ, respectively. The terms Q_{xx}-Q_{zz} and Q_{yy}-Q_{zz} show this anisotropy. In general, the quadrupole moment tensor components show only a modest dependency

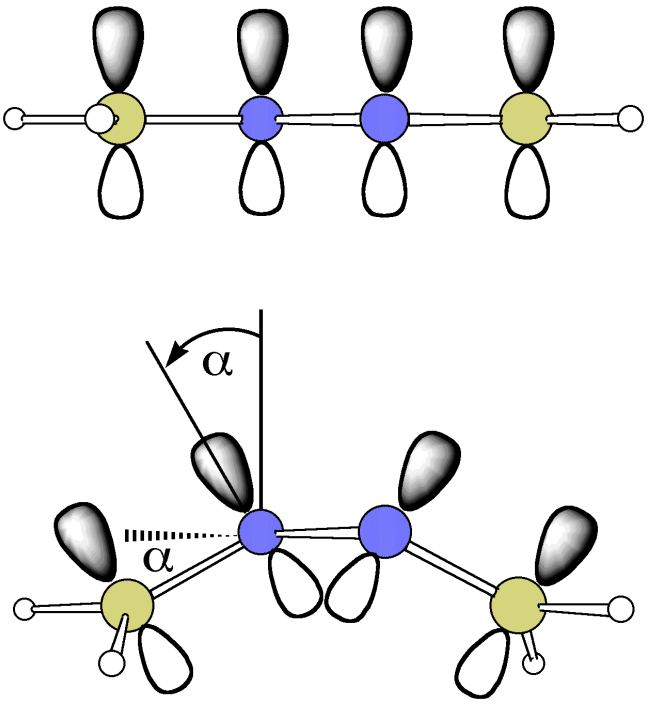

Scheme 4 *The* C_2 *distortion of formaldazine into* gauche *conformations with ∠(C-N-N-C) dihedral angles* τ *leads to a rotation of the p-orbitals used in the CN double bonds by an angle* $\alpha = 0.5 \cdot (180^o - \tau)$

on the theoretical level. Yet, the theoretical model dependency is systematic and significant in that the choice of basis set is more important than the application of advanced methods for electron correlation. The Q_{zz} data show that a more flexible basis set increases Q_{zz} no matter what theoretical method is used. For a given basis set, correlation effects present only a minor correction. Thus, the Q_{zz} value computed at RHF/6-311G** is superior to the value computed at QCISD/6-31G* and an excellent approximation to the QCISD/6-311G** value.

Conformational effects on the quadrupole moment tensor components of formaldazine

There are some clear trends in the variations of the quadrupole moment tensor components of formaldazine with variations in the conformation about the N-N bond. The data in Tables 7 - 10 show a decrease of Q_{zz} and a less pronounced increase of Q_{yy} as the azine conformation deviates more and more from the *trans* conformation. We use the angle α to describe these conformational changes. The angle α is half of the difference between 180° and the ∠(C-N-N-C) dihedral angle. Suppose that the conformational changes occur without major electronic relaxation. In this case, one would expect that the change in the quadrupole moment tensor component Q_{zz} reflects primarily the change in the $\langle r_i^2 \rangle$ term caused by the rotation (Scheme 4). For the component that is due to the p-orbital contributions (indicated by the prime in the notation) and for small α angles, one can then expect that

$$Q_{zz}(\alpha)' = Q_{zz}(0)' \cdot \cos^2(\alpha) \quad (4)$$

and for the change one obtains

$$Q_{zz}(0)' - Q_{zz}(\alpha)' = Q_{zz}(0)' \cdot [1 - \cos^2(\alpha)] = Q_{zz}(0)' \cdot \sin^2(\alpha) \quad (5.1)$$

$$Q_{yy}(0)' - Q_{yy}(\alpha)' = Q_{zz}(0)' \cdot \sin^2(\alpha) \quad (5.2)$$

Since $Q_{zz}(0)'$ is only a part of $Q_{zz}(0)$, the changes due to the rotation of the p-orbitals should be reduced by a factor P so that one obtains the equations

$$\Delta Q_{zz} = Q_{zz}(0) - Q_{zz}(\alpha) = P \cdot Q_{zz}(0)' \cdot \sin^2(\alpha) \quad (6.1)$$

$$\Delta Q_{yy} = Q_{yy}(0) - Q_{yy}(\alpha) = P \cdot Q_{zz}(0)' \cdot \sin^2(\alpha) \quad (6.2)$$

In Figure 2 we have examined the validity of these equations. The linear function $25.631 \cdot \sin^2(\alpha)$ in Figure 2 emphasizes that Q_{zz}' is only a part of Q_{zz}. Importantly, we find that the variations of ΔQ_{zz} and ΔQ_{yy} are indeed linear with $\sin^2(\alpha)$ and the slopes are 4.002 and 6.191, respectively. What is the origin of this significant difference in the slopes? If ΔQ_{yy} grows faster than ΔQ_{zz} decreases, then the orbital rotation cannot be the only conformational effect on the quadrupole moments. What additional mechanism could be operative? We carried out an NBO analysis to examine elec-

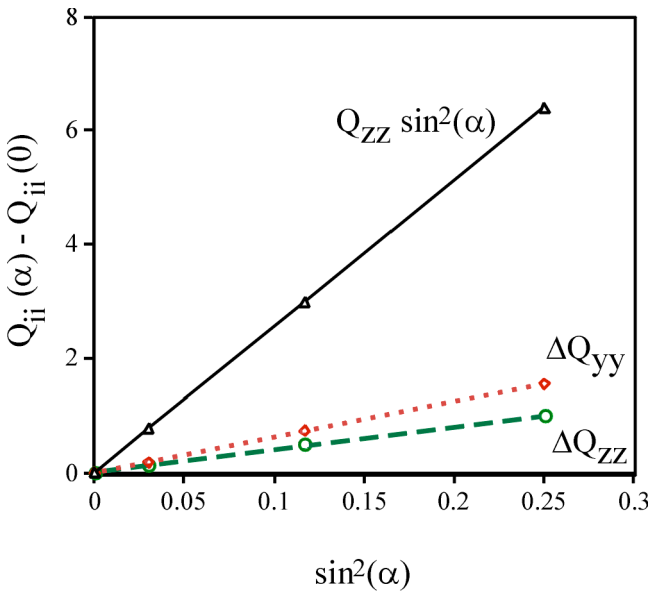

Figure 2 *Changes of the quadrupole moment tensor components* Q_{zz} *and* Q_{yy} *as a function of* $\sin^2(\alpha)$*. The angle* α *is half of the difference between 180° and the ∠(C-N-N-C) dihedral angle*

tron density relaxation effects associated with conformational change and the results are summarized in Table 11. The reduction of the τ-dihedral angle leads to a small decrease of the CN bond polarity which is essentially due to a shift of the CN π-type electron density. This small transfer of electron density from N to C is magnified in Q_{yy} because the electron density transfer increases the distance from the molecular center of nuclear charge and this distance enters the equation for Q_{yy} in quadratic form.

Conclusion

Formaldazine is a quadrupolar molecule with primitive quadrupole moment tensor components of Q_{xx} = -22.4, Q_{yy} = -20.4 and Q_{zz} = -25.6 DÅ at the theoretical level QCISD/6-311++G**. The examination of the theoretical level dependency shows that the reliable computation of a quadrupole moment requires the use of a flexible basis set. A large part of the component Q_{zz} = -25.6 DÅ is due to the π-system and compares, on a per electron basis, with the Q_{zz} value of benzene. Conformational changes of the azines in the range $120^o < \tau < 180^o$ have but a minute effect on the energy and are associated with only minor electronic relaxation. In particular, these conformational changes alter the quadrupole moment tensor components less than ΔQ_{xx} = +0.4, ΔQ_{yy} = +1.6 and ΔQ_{zz} = -1.0 DÅ at QCISD/6-311++G**//QCISD/6-31G*. The direction of these changes has been explained by consideration of the rotation of the CN-π-systems and a small reduction of the CN bond polarity in the *gauche* structures.

The Q_{zz} component of formaldazine is representative of the quadrupole moment tensor component along the direction of the C_2 axis of the azine bridge as such. Hence, the results of this theoretical and computational study suggest that azines can engage in strong quadrupole-quadrupole interactions. Current research in our group is directed at the study of azine-azine and azine-arene interactions by way of a synergistic combination of experimentation, theory and computation.

Acknowledgments We thank Research Support Computing branch of the MU IAT Services for generous support. M. L. thanks the Natural Sciences and Engineering Research Council of Canada for a Post-Graduate Scholarship, Type B.

Supplemental material available The electronic version of this article includes pdb files of all stationary structures.

References

1. Pu, L. S. *J. Chem. Soc., Chem. Commun.* **1991**, 429.
2. Oudar, J. L.; Hierle, R. *J. Appl. Phys.* **1977**, *48*, 2699.
3. Sagawa, M.; Kagawa, H.; Kakuta, A.; Kaji, M.; Saeki, M.; Namba, Y. *Nonlinear Opt.* **1996**, *15*, 147.
4. Zyss, J.; Ledoux, I.; Bertault, M.; Toupet, E. *Chem. Phys.* **1991**, *150*, 125.
5. (a) Lewis, M.; Barnes, C. L.; Glaser, R. *Acta Crystallogr., Sect. C*, **1999**, *55*, in press. (b) Chen, G. S.; Wilbur, J. K.; Barnes, C. L.; Glaser, R. *J. Chem. Soc., Perkin Trans. 2* **1995**, 2311.
6. (a) Lewis, M.; Barnes, C.; Hathaway, B. A.; Glaser, R. *Acta Crystallogr. Sect. C* **1999**, *55*, 975. (b) Lewis, M.; Barnes, C. L.; Glaser, R. *Can. J. Chem.* **1998**, *76*, 1371.
7. Steiger, D.; Ahlbrandt, C.; Glaser, R. *J. Phys. Chem. B* **1998**, *102*, 4257.
8. We have studied the arene-arene contacts in unsymmetrical azines (refs. 5 and 6) and also in symmetrical azines, see: (a) Lewis, M.; Barnes, C. L.; Glaser, R. *J. Chem. Crystallogr.*, submitted. (b) Chen, G. S.; Anthamatten, M.; Barnes, C. L.; Glaser, R. *J. Org. Chem.* **1994**, *59*, 4336. (c) Chen, G. S.; Anthamatten, M.; Barnes, C. L.; Glaser, R. *Angew. Chem., Int. Ed. Engl.* **1994**, *33*, 1081.
9. Glaser, R.; *et al*., to be published.
10. Williams, J. H. *Acc. Chem. Res.* **1993**, *26*, 593.
11. Hobza, P.; Selzle, H. L.; Schlag, E. W. *Chem. Rev.* **1994**, *94*, 1767.
12. Spackman, M. A. *Chem. Rev.* **1992**, *92*, 1769.
13. (a) Price, S. L.; Stone, J. A. *J. Chem. Phys.* **1987**, *86*, 2859. (b) Jorgensen, W. L.; Severance, D. L. *J. Am. Chem. Soc.* **1990**, *112*, 4768. (c) Hunter, C. A. *Angew. Chem., Int. Ed. Engl.* **1993**, *32*, 1584.
14. (a) Szabo, A.; Ostlund, N. S. *Modern Quantum Chemistry: Introduction to Advanced Electronic Structure Theory*; MacMillan Publishing: New York, 1982. (b) Hehre, W. L.; Radom. L.; Schleyer, P. v. R.; Pople, J. A. *Ab Initio Molecular Orbital Theory*; Wiley & Sons: New York, 1986.
15. (a) Head-Gordon, M.; Pople, J. A.; Raghavachari, K. *J. Chem. Phys.* **1987**, *87*, 5968. (b) Hampel, C.; Peterson, K. A.; Werner, H.-J. *Chem. Phys. Lett.* **1992**, *120*, 1.
16. 6-31G* and 6-31G**: (a) Hehre, W. J.; Ditchfield, R.; Pople, J. A. *J. Chem. Phys.* **1972**, *56*, 2257. (b) Francl, M. M.; Petro, W. J.; Hehre, W. J.; Binkley, J. S.; Gordon, M. S.; DeFrees, D. J.; Pople, J. A. *J. Chem. Phys.* **1982**, *77*, 3654. (c) Hariharan, P. C. Pople, J. A. *Theor. Chim. Acta* **1973**, *28*, 213.
17. 6-311G**: (a) Krishnan, R.; Binkley, J. S.; Seeger, R.; Pople, J. A. *J. Chem. Phys.* **1980**, *72*, 650. (b) McLean, A. D.; Chandler, G. S. *J. Chem. Phys.* **1980**, *72*, 5639.
18. Diffuse functions: Clark, T.; Chandrasekhar, J.; Schleyer, P. v. R. *J. Comput. Chem.* **1983**, *4*, 294.
19. (a) Glendening, E. D.; Reed, A. E.; Carpenter, J. E.; Weinhold, F. *NBO Version 3.1*. (b) Glendening, E. D.; Weinhold, F. *J. Comput. Chem.* **1998**, *19*, 628, and references cited therein.
20. Gaussian 94, Revision C.3; Frisch, M. J.; Trucks, G. W.; Schlegel, H. B.; Gill, P. M. W.; Johnson, B. G.; Robb, M. A.; Cheeseman, J. R.; Keith, T.; Petersson, G. A.; Montgomery, J. A.; Raghavachari, K.; Al-Laham, M. A.; Zakrzewski, V. G.; Ortiz, J. V.; Foresman, J. B.; Cioslowski, J.; Stefanov, B. B.; Nanayakkara, A.; Challacombe, M.; Peng, C. Y.; Ayala, P. Y.; Chen, W.; Wong, M. W.; Andres, J. L.; Replogle, E. S.; Gomperts, R.; Martin, R. L.; Fox, D. J.; Binkley, J. S.; Defrees, D.

J.; Baker, J.; Stewart, J. P.; Head-Gordon, M.; Gonzalez, C.; Pople , J. A. Gaussian Inc.: Pittsburgh, PA. 1995.
21. (a) Ogilvie, J. F.; Cole, K. C. *Spectrochim. Acta, Part A* **1971**, *27*, 877. (b) Bondybey, V. E.; Nibler, J. W. *Spectrochim. Acta, Part A* **1973**, *29*, 645.
22. Hagen, K.; Bondybey, V.; Hedberg, K. *J. Am. Chem. Soc.* **1977**, *99*, 1365.
23. (a) Harris, W. C.; Yang, D. B.; Wilcox, P. M. *Spectrochim. Acta, Part A* **1975**, *31*, 1981. (b) Kirste, K.; Poppek, R.; Rademacher, P. *Chem. Ber.* **1984**, *117*, 1061.
24. Skancke, A. *J. Mol. Struct.* **1976**, *34*, 291.
25. Bock, C. W.; George, P.; Trachtman, M. *J. Comput. Chem.* **1984**, *5*, 395.
26. Bachrach, S. M.; Liu, M. *J. Am. Chem. Soc.* **1991**, *113*, 7929.
27. Oberhammer, H.; Bauknight, C. W., Jr., DesMarteau, D. D. *Inorg. Chem.* **1989**, *28*, 4340.
28. Wiberg, K. B.; Rablen, P. R.; Marquez, M. *J. Am. Chem. Soc.* **1992**, *114*, 8654.
29. Glaser, R.; Chen, G. S.; Barnes, C. L. *J. Org. Chem.* **1993**, *58*, 7446, and references cited there.
30. Glaser, R.; Chen, G. S. *J. Comput. Chem.* **1998**, *19*, 1130.
31. (a) Benzene shows a charge separation of 0.235 for the C-H bond with the H-atom being the positive pole. (b) Glaser, R.; Nichols, G. R. *J. Org. Chem.*, submitted.
32. Hathaway, B.; Day, D.; Lewis, M.; Glaser, R. *J. Chem. Soc, Perkin Trans. 2* **1998**, 2713.
33. For *ab initio* studies of the quadrupole moment of benzene, see: Ha, T.-K. *Chem. Phys. Lett.* **1981**, *79*, 313. (b) Dougherty, D. A. *Science* **1996**, *271*, 163.